RESEARCH ARTICLE

Differences in pathological changes between two rat models of severe traumatic brain injury

Yi-Ming Song[1, 2], Yu Qian[1, 2], Wan-Qiang Su[1, 2], Xuan-Hui Liu[1, 2], Jin-Hao Huang[1, 2], Zhi-Tao Gong[1, 2], Hong-Liang Luo[1, 2], Chuang Gao[1, 2], Rong-Cai Jiang[1, 2, *]

1 Department of Neurosurgery, General Hospital, Tianjin Medical University, Tianjin, China
2 Key Laboratory of Injuries, Variations and Regeneration of Nervous System, Tianjin Neurological Institute, Tianjin, China

Funding: *This study was supported by the National Natural Science Foundation of China, No. 81671221 (to RCJ).*

Graphical Abstract

Similarities and differences between rat models of severe controlled cortical impact and severe free weight drop

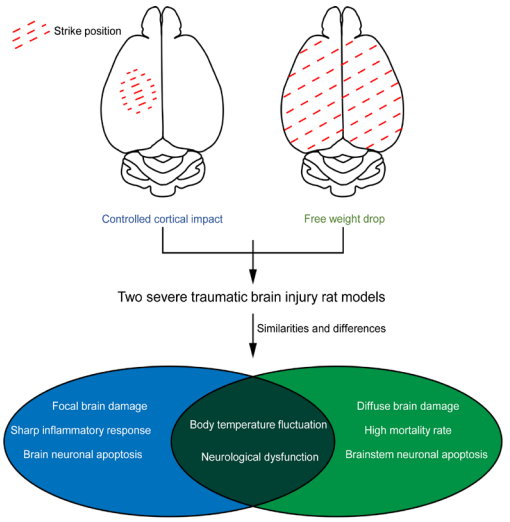

***Correspondence to:**
Rong-Cai Jiang, PhD,
jiang116216@163.com.

orcid:
0000-0002-9119-0115
(Rong-Cai Jiang)

doi: *10.4103/1673-5374.257534*

Received: *November 14, 2018*
Accepted: *April 10, 2019*

Abstract

The rat high-impact free weight drop model mimics the diffuse axonal injury caused by severe traumatic brain injury in humans, while severe controlled cortical impact can produce a severe traumatic brain injury model using precise strike parameters. In this study, we compare the pathological mechanisms and pathological changes between two rat severe brain injury models to identify the similarities and differences. The severe controlled cortical impact model was produced by an electronic controlled cortical impact device, while the severe free weight drop model was produced by dropping a 500 g free weight from a height of 1.8 m through a plastic tube. Body temperature and mortality were recorded, and neurological deficits were assessed with the modified neurological severity score. Brain edema and blood-brain barrier damage were evaluated by assessing brain water content and Evans blue extravasation. In addition, a cytokine array kit was used to detect inflammatory cytokines. Neuronal apoptosis in the brain and brainstem was quantified by immunofluorescence staining. Both the severe controlled cortical impact and severe free weight drop models exhibited significant neurological impairments and body temperature fluctuations. More severe motor dysfunction was observed in the severe controlled cortical impact model, while more severe cognitive dysfunction was observed in the severe free weight drop model. Brain edema, inflammatory cytokine changes and cortical neuronal apoptosis were more substantial and blood-brain barrier damage was more focal in the severe controlled cortical impact group compared with the severe free weight drop group. The severe free weight drop model presented with more significant apoptosis in the brainstem and diffused blood-brain barrier damage, with higher mortality and lower repeatability compared with the severe controlled cortical impact group. Severe brainstem damage was not found in the severe controlled cortical impact model. These results indicate that the severe controlled cortical impact model is relatively more stable, more reproducible, and shows obvious cerebral pathological changes at an earlier stage. Therefore, the severe controlled cortical impact model is likely more suitable for studies on severe focal traumatic brain injury, while the severe free weight drop model may be more apt for studies on diffuse axonal injury. All experimental procedures were approved by the Ethics Committee of Animal Experiments of Tianjin Medical University, China (approval No. IRB2012-028-02) in February 2012.

Key Words: *nerve regeneration; severe traumatic brain injury; animal model comparison; free weight drop; controlled cortical impact; neurological impairment; neuroinflammation; blood-brain barrier damage; neuronal apoptosis; diffuse axonal injury; brainstem injury; neural regeneration*

Chinese Library Classification No. *R447; R361*

Introduction

Traumatic brain injury (TBI) often leads to structural and functional changes (Mateo and Porter, 2007; Gerbatin et al., 2017), and these changes are more pronounced in severe TBI. Therefore, studying the pathological mechanisms of severe TBI is the key to the development of effective and safe treatments.

For over a century, numerous animal models of TBI have been used to study the pathological mechanisms and to develop novel therapies (Osier and Dixon, 2016a). The three most popular rodent models of TBI are the controlled cortical impact (CCI), free weight drop (FWD) and fluid percussion injury models. CCI was developed in the late 1980s, and produces severe TBI with set impact parameters (Osier and Dixon, 2016b). Another advantage of CCI is that it only needs one surgical procedure, as opposed to standard fluid percussion injury, which requires two. The FWD rat model, proposed by Anthony Marmarou in 1994 (Marmarou et al., 1994), aims to reproduce diffuse axonal injury. Diffuse axonal injury is one of the most severe and destructive types of TBI, resulting from acceleration, deceleration or rotational injuries (Buki and Povlishock, 2006; Ogata, 2007).

Although there are various models of severe TBI, none fully reproduces human TBI, and each model has its own characteristics that correspond to specific clinical TBI features (Povlishock, 2016). For example, CCI mimics focal TBI, while FWD mimics diffuse TBI (Ma et al., 2019). A number of studies have compared the pathological features of CCI and FWD, including changes in intracranial pressure (Clausen and Hillered, 2005) and neutrophil aggregation (Clark et al., 1994). However, severe brain injuries produced by these methods have not yet been compared. Currently, it is difficult to choose the model that best reproduces the pathological changes of severe TBI. When severe TBI is induced, a variety of pathological changes occur, including neurological dysfunction, brain edema, brain vascular dysfunction, inflammatory response and cell death (Corps et al., 2015; Jullienne et al., 2016; Cui et al., 2017; Obenaus et al., 2017).

In this study, we examine the characteristics of severe TBI produced by CCI and FWD, and we describe the similarities and differences in the pathological changes.

Materials and Methods

Animals

A total of 164 adult male Sprague-Dawley rats, weighing 250–300 g and 8 weeks of age, were purchased from the Military Medical Academy of China (Beijing, China) (approval number: SCXK (Jing) 2014-0004). All rats were housed in the animal facilities of Tianjin Medical University General Hospital with sufficient food and water supply. The experimental protocols were approved by the Ethics Committee of Animal Experiments of Tianjin Medical University, China (approval No. IRB2012-028-02) in February 2012.

Rats (n = 164) were randomly divided into three groups. In the sham group (n = 24), rats received all procedures except CCI or FWD. In the severe CCI (sCCI) group (n = 60), the rats were subjected to CCI with the striking device. In the severe FWD (sFWD) group (n = 80), a 500 g free weight was dropped from a height of 1.8 m. The timeline of the experimental protocols and assessments is shown in **Figure 1**.

sCCI model

Rats (n = 60) were weighed and intraperitoneally anesthetized with 10% chloral hydrate, 3 mL/kg (Department of General Medical Laboratory, Tianjin Medical University, Tianjin, China). After anesthesia, rats were fixed on the stereotactic frame, followed by trimming and disinfecting the scalp. After a midline scalp incision was made, a 6 mm diameter hole was drilled in the left parietal bone. The impounder tip of the striking device (electronic CCI model device 6.3, Custom Design & Fabrication, Sandston, VA, USA) was extended through the skull hole and positioned near the dura surface (Kulbe et al., 2018). The impact parameters were as follows: speed, 3.5 m/s; dwell time, 500 ms; and striking depth, 2.2 mm. Noticeable cerebral cortical contusion in rats was considered successful modeling. After injury, the scalp incision was sutured and the rats were monitored carefully until they awoke.

sFWD model

The sFWD rat model was produced according to a previously described method, with minor modification (Marmarou et al., 1994; Chen et al., 2018). In brief, rats (n = 80) were weighed and intraperitoneally anesthetized with 10% chloral hydrate, 3 mL/kg. After trimming and disinfecting the scalp, the surgical site incision was made to expose the surface of the skull. A steel disc, 10 mm in diameter and 3 mm thick, was fixed in the center of the skull. Next, the rats were placed in the prone position on a foam bed. Subsequently, a 500 g weight was made to fall freely through a plastic guide positioned directly above the cranium from a height of 1.8 m. Immediately after the impact, all items were removed to avoid secondary impact. Visible limb twitching or stiffness was considered successful modeling. After injury, the scalp incision was closed, and the rats were carefully monitored until they regained consciousness.

Body temperature and mortality

Rat body temperatures (pre-injury, and 1, 24, 48 and 72 hours post-injury) were measured with a thermometer. Mortality within 72 hours after injury was recorded.

Modified neurological severity score (mNSS)

Neurological functions were assessed at 24 and 72 hours after injury with the mNSS, as described previously (Gao et al., 2017). The mNSS score ranged from 0 to 18 and the mNSS was performed by four tests: motor test, sensory test, balance beam test, and reflex test (**Table 1**). A higher score indicates greater neurological impairment.

Brain water content

According to a method described previously (Su et al., 2014),

Table 1 mNSS protocols

mNSS experimental parameters	Scores
Motor tests	
Raising rat by the tail	
Flexion of the forelimb	1
Flexion of the hindlimb	1
Head deviating from the vertical axis by > 10° within 30 s	1
Placing rat on the floor	
Normal walking	0
Incapability to walk straight	1
Turning to the paralyzed side	2
Falling down to the paralyzed side	3
Sensory tests	
Placement test (visual and tactile test)	1
Proprioception test (squeezing the claws to the table edge to stimulate the limb muscles)	2
Balance beam tests	
Stable balance posture	0
Grasping edge of the beam	1
Holding the beam, one limb falling from the beam	2
Holding the beam and two limbs falling from the beam or rotating on the beam (> 60 s)	3
Trying to balance on the beam but falling (> 40 s)	4
Trying to balance on the beam but falling (> 20 s)	5
Falling, not trying to balance on the beam (< 20 s)	6
Reflexes absent and abnormal movements	
Auricle reflex (shaking head when touching the external auditory canal)	1
Corneal reflex (blinking when tapping the cornea with cotton)	1
Panic reflex (motor response to the noise from snapping a cardboard)	1
Epilepsy, myoclonus, dystonia	1
Total scores	18

mNSS: Modified Neurological Severity Score; s: seconds.

brain water content was measured 72 hours after severe TBI. Briefly, after anesthesia, brains were harvested after perfusion with phosphate-buffered saline (PBS). The wet weights were measured with an electronic analytical balance immediately after removal. The brain was dried at 100°C for 24 hours, and the dry weight was obtained in the same manner. Brain water content (%) was calculated as: (wet weight – dry weight)/wet weight × 100%.

Blood-brain barrier damage

Blood-brain barrier damage was assessed by Evans blue (E8010, Solarbio, Beijing, China) extravasation 72 hours after injury (Lin et al., 2017). Under deep anesthesia, 2% Evans blue dissolved in PBS was administered through the femoral vein (5 mL/kg) and allowed to circulate for 30 minutes. The animals were then transcardially perfused with PBS, and the brains were removed for observation.

Cytokine array

The inflammatory response was evaluated using the Rat Cytokine Array Panel A (ARY008, R&D Systems, Minneapolis, MN, USA). This kit measures the following 29 cytokines that are associated with the inflammatory response: Cytokine-induced neutrophil chemoattractant-1 (CINC-1), cytokine-induced neutrophil chemoattractant-2α (CINC-2α), cytokine-induced neutrophil chemoattractant-3 (CINC-3), ciliary neurotrophic factor (CNTF), fractalkine (CX3CL1), soluble intercellular adhesion molecule-1 (sICAM-1), granulocyte-macrophage colony stimulating factor (GM-CSF), interferon-γ (IFN-γ), interleukin-1α (IL-1α), interleukin-1β (IL-1β), interleukin-1ra (IL-1ra), interleukin-2 (IL-2), interleukin-3 (IL-3), interleukin-4 (IL-4), interleukin-6 (IL-6), interleukin-10 (IL-10), interleukin-13 (IL-13), interleukin-17 (IL-17), interferon-inducible protein-10 (IP-10), little isoxanthopterin (LIX), L-selectin, C-X-C motif chemokine ligand 9 (CXCL9), macrophage inflammatory protein-1α (MIP-1α), macrophage inflammatory protein-3α (MIP-3α), RANTES (CCL5), thymus chemokine (CXCL7), tissue inhibitor of metalloproteinase-1 (TIMP-1), tumor necrosis factor-a (TNF-a), and vascular endothelial growth factor (VEGF). Following transcardial perfusion with PBS 72 hours after injury, a 130 mg brain tissue sample from the pericontusional cortex was extracted and homogenized in PBS with protease inhibitors. After homogenization, Triton X-100 was added to a concentration of 1% and frozen at −80°C. The samples were then thawed and centrifuged at 10,000 × *g* for 5 minutes to remove cellular debris. Before measurements, total protein concentrations of samples were quantified using the Bicinchoninic Acid Protein Assay Kit (23227, Thermo Fisher Scientific, Waltham, MA, USA) according to the manufacturer's instructions. Background gray values were removed to reduce differences between groups, and gray values for the sham group were used as a reference for the other two groups. Cytokine levels were calculated based on the mean gray value with ImageJ software (Version 1.52a, NIH, Bethesda, MD, USA). For each cytokine, relative gray value was equal to the mean gray value in the sCCI or sFWD group/mean gray value in the sham group.

Hematoxylin-eosin staining

To observe the histology of the injured brains, hematoxylin-eosin staining was conducted as described previously 72 hours after injury (Dai et al., 2018). The brains were perfused with PBS and then fixed in 4% paraformaldehyde for 24 hours. The tissue was dehydrated through a graded alcohol series, permeabilized with xylene, embedded in paraffin, and then sliced into serial coronal sections at 7 μm intervals. These sections were stained with hematoxylin and eosin (G1120, Solarbio, Beijing, China). Lesions (three sections per group) were observed under the microscope (ECLIPSE 80i, Nikon, Tokyo, Japan).

Terminal deoxynucleotidyl transferase-mediated dUTP nick end labeling (TUNEL) staining

To assess brain and brainstem tissue apoptosis, TUNEL immunofluorescent staining was performed 72 hours after injury. Paraffin sections were prepared as described above and stained using the DeadEnd™ Fluorometric TUNEL Sys-

tem (G3250, Promega, Madison, WI, USA) according to the manufacturer's instructions. After staining, paraffin sections were counterstained with 4′,6-diamidino-2-phenylindole (DAPI; Abcam, Cambridge, UK). TUNEL-positive cells around the lesion were observed in three slides for each group, with each slide containing six fields, under a fluorescence microscope (BX53, Olympus, Tokyo, Japan). Data are presented as the percentage of apoptotic cells (TUNEL-positive cells/DAPI-stained cells).

Statistical analysis

Data are expressed as the mean ± SD and were analyzed by one-way analysis of variance followed by the Bonferroni *post hoc* test, independent-sample *t*-test, or chi-square test using SPSS software (Version 25, IBM, Armonk, NY, USA). A value of $P < 0.05$ was considered statistically significant.

Results

Changes in vital signs and neurological impairment

Among the 60 sCCI rats, 83.3% survived. Among the 80 sFWD rats, only 67.5% survived. The survival rate was significantly higher in the sCCI group than in the sFWD group ($P < 0.05$, chi-square test). Compared with the sham group, body temperatures decreased at 1 hour post-injury in the sCCI and sFWD groups. The body temperature in rats with severe TBI rose sharply by 24 hours post-injury, but returned to normal at 48 hours post-injury (**Figure 2A**). mNSS scores were higher in the sCCI and sFWD groups compared with the sham group at 24 and 48 hours (**Figure 2B**). However, there were no significant differences in body temperature or neurological function between the sCCI and sFWD groups. Furthermore, we compared each test parameter (motor, sensory, balance beam, and reflex) score in the mNSS at 24 and 72 hours post injury. Differences were detected only in the motor and balance beam tests between the sham and the sCCI and sFWD groups. No significant differences were found in the motor and balance beam tests between the sCCI and sFWD groups 24 hours after injury (**Figure 2C**). At 72 hours, there were significant differences in the motor and balance beam tests between the sCCI and sham groups, and a significant difference was detected in the balance beam test between the sFWD and sham groups. In addition, at 72 hours, balance beam test scores were improved in the sCCI group compared with the sFWD group (**Figure 2D**).

Brain edema and blood-brain barrier damage

sCCI not only produced significant brain edema compared with the sham group at 72 hours after injury, but also in comparison with the sFWD group. Brain edema was not severe in the sFWD group and failed to induce significant differences, compared with the sham group (**Figure 3A**). Blood-brain barrier damage was evaluated by observing Evans blue staining in the whole brain after intravenous injection. Blue staining was not detected in the sham rats, but was visible in the cortical impact site in sCCI rats. Evans blue leakage in the sFWD group was observed from the cerebral surface to the cerebellum and brainstem (**Figure 3B**). This analysis suggests that the blood-brain barrier lesion was focal in sCCI rats, but diffuse in sFWD rats.

Cytokine levels

Of the 29 inflammatory cytokines tested, 10 were significantly upregulated in the sCCI group compared with the sFWD group, including CINC-1, CINC-2α, CNTF, CX3CL1, sICAM-1, IL-1ra, L-selectin, MIP-1α, CXCL7 and TIMP-1 (**Figure 4A** and **B**). The levels of these 10 cytokines in the sCCI and sFWD groups relative to the sham group are shown in **Table 2**.

Table 2 Cytokine gray value ratios of sCCI and sFWD groups

Cytokines	sCCI	sFWD
CINC-1	1.75±0.02$^{\#\#\#}$	1.02±0.05
CINC-2α	3.09±0.03$^{\#\#\#}$	0.97±0.03
CNTF	3.01±0.02$^{\#\#\#}$	1.17±0.02
CX3CL1	2.53±0.05$^{\#\#\#}$	1.09±0.01
sICAM-1	1.96±0.06$^{\#\#\#}$	1.01±0.04
IL-1ra	2.07±0.03$^{\#\#\#}$	1.00±0.04
L-selectin	2.70±0.02$^{\#\#\#}$	1.01±0.03
MIP-1α	2.05±0.01$^{\#\#\#}$	1.00±0.03
CXCL7	2.86±0.03$^{\#\#\#}$	1.15±0.08
TIMP-1	3.00±0.12$^{\#\#\#}$	1.07±0.01

Cytokine gray value ratios = mean gray value of each cytokine in sCCI or sFWD group/mean gray value of the corresponding cytokine in sham group. Data are expressed as the mean ± SD ($n = 5$; independent-sample *t* test). ###$P < 0.001$, *vs.* sFWD group. sCCI: Severe controlled cortical impact; sFWD: severe free weight drop; CINC-1: cytokine-induced neutrophil chemoattractant-1; CINC-2α: cytokine-induced neutrophil chemoattractant-2α; CNTF: ciliary neurotrophic factor; CX3CL1: fractalkine; sICAM-1: soluble intercellular adhesion molecule-1; IL-1ra: interleukin-1ra; MIP-1α: macrophage inflammatory protein-1α; CXCL7: thymus chemokine 7; TIMP-1: tissue inhibitor of metalloproteinase-1.

Lesion characteristics and neuronal apoptosis

The traumatic lesions in sCCI rats were localized to the impact site in the left cerebral hemisphere. In comparison, the sFWD rats showed diffuse swelling on the brain surface, extensive subdural hemorrhage and subarachnoid hemorrhage, and scattered hemorrhage from the cerebral surface to the cerebellum and brainstem (**Figure 5A**). The traumatic lesion in the sCCI group was visible under a microscope in hematoxylin-eosin-stained brain sections, while there was no visible lesion in the sham and sFWD groups (**Figure 5B**). TUNEL-positive cells were most numerous in the cerebral cortex in the sCCI group compared with the sham and sFWD groups. Only a few TUNEL-positive cells were detected in the sham group (**Figure 5C**). The percentage of apoptotic cells was increased markedly in the sCCI and sFWD groups. In addition, apoptotic cells were increased in the cortex in the sCCI group compared with the sFWD group (**Figure 5D**). Furthermore, apoptotic cells were numerous in the brainstem in sFWD rats. TUNEL-positive cells were few in the sham and sCCI rats (**Figure 5E**). The number of TUNEL-positive cells was significantly different between the sFWD and sCCI groups (**Figure 5F**).

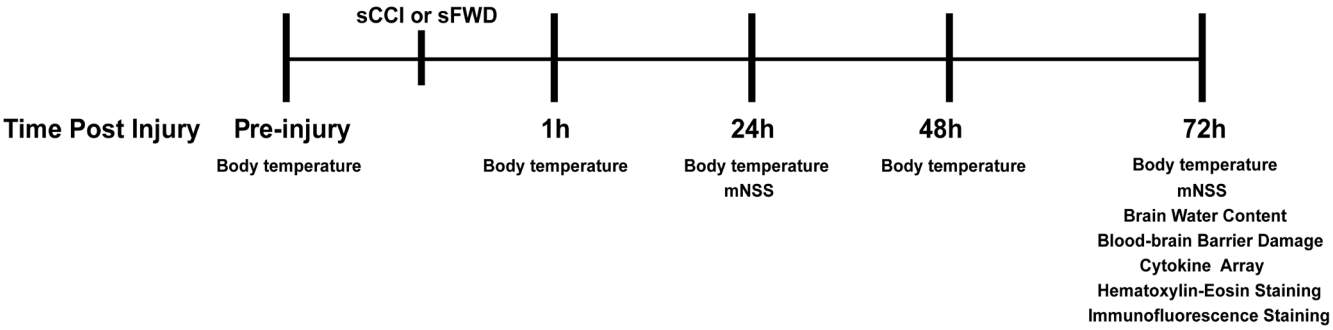

Figure 1 Timeline of the experimental procedures.
sCCI: Severe controlled cortical impact; sFWD: severe free weight drop; mNSS: modified neurological severity score; h: hour(s).

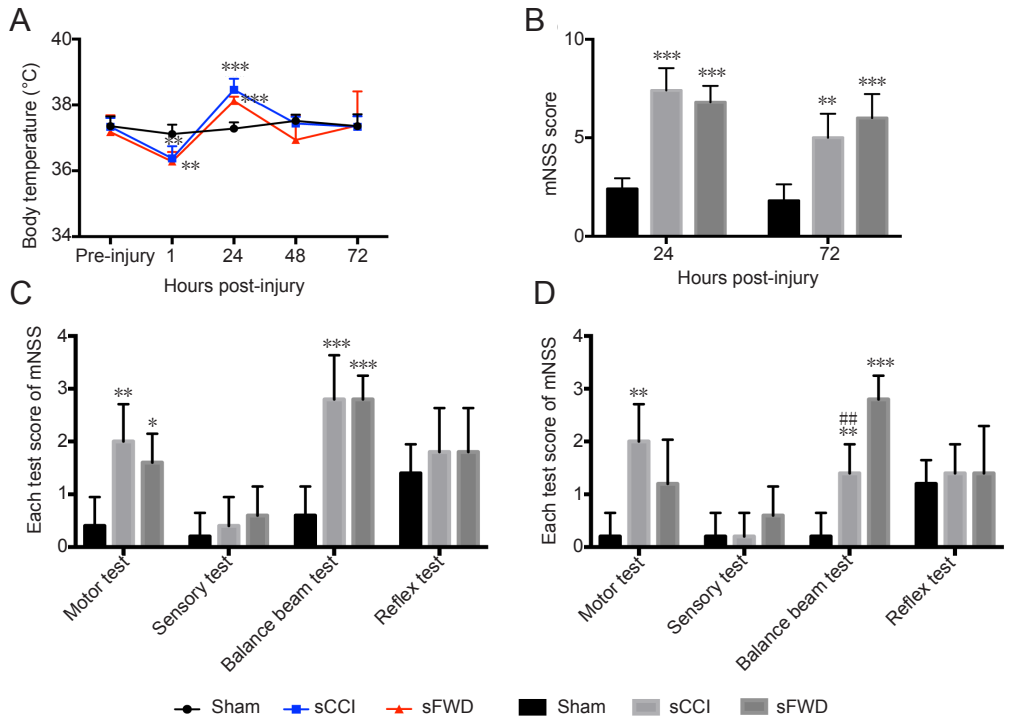

Figure 2 Body temperature fluctuation and neurological function in rats.
Changes in body temperature pre-injury and post-injury (A), and neurological impairments measured with the mNSS at 24 and 72 hours after injury (B). Motor, sensory, balance beam and reflex tests in the mNSS at 24 hours (C) and 72 hours (D) after injury. Data are expressed as the mean ± SD (n = 5; one-way analysis of variance with the Bonferroni *post hoc* test). $*P < 0.05$, $**P < 0.01$, $***P < 0.001$, *vs.* sham group; $\#\#P < 0.01$, *vs.* sFWD group. sCCI: Severe controlled cortical impact; sFWD: severe free weight drop; mNSS: modified neurological severity score.

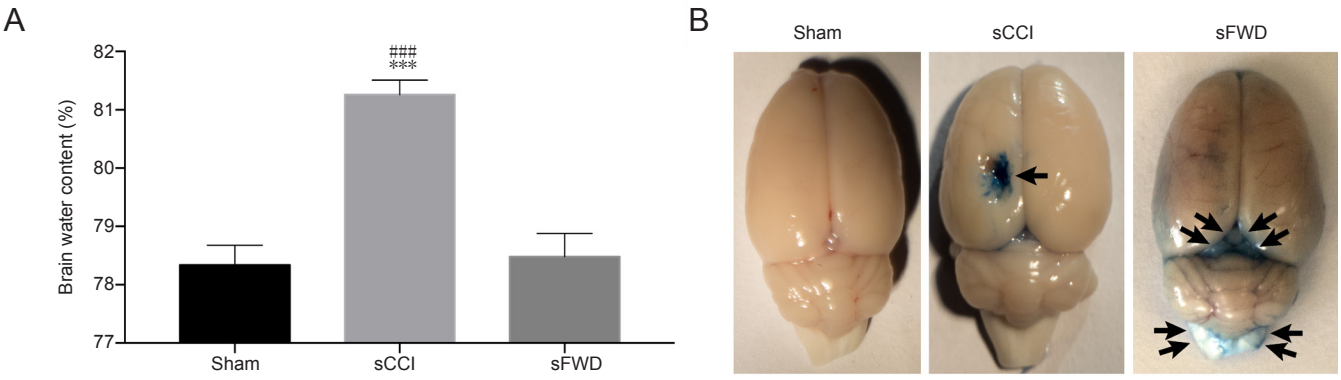

Figure 3 Brain edema and blood-brain barrier damage in the three groups.
(A) Brain water content; (B) Evans blue extravasation raw images at 72 hours after injury. Arrows indicate areas of visible Evans blue leakage. Data are expressed as the mean ± SD (n = 5; one-way analysis of variance with Bonferroni *post hoc* test). $***P < 0.001$, *vs.* sham group; $\#\#\#P < 0.001$, *vs.* sFWD group. sCCI: Severe controlled cortical impact; sFWD: severe free weight drop.

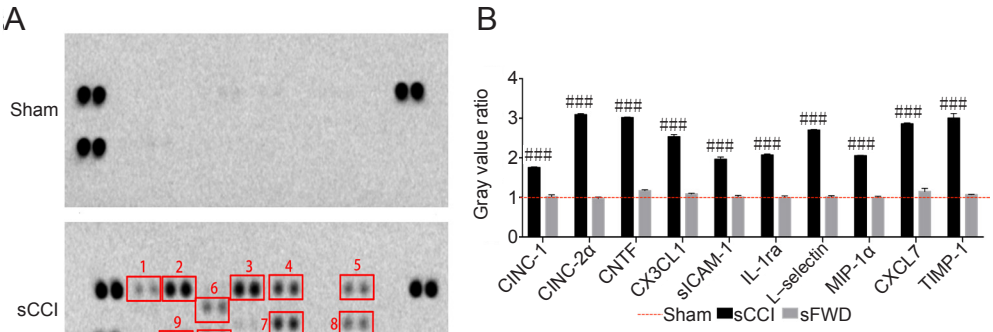

Figure 4 Inflammatory response at 72 hours after injury.
(A) Inflammatory cytokine expression levels in the three groups. (B) Quantitative analysis of the 10 cytokines. 1–10 in (A) represents CINC-1, CINC-2α, CNTF, CX3CL1, sICAM-1, IL-1ra, L-selectin, MIP-1α, CXCL7 and TIMP-1, respectively. Cytokine gray value ratios = mean gray value of each cytokine in sCCI or sFWD group/mean gray value of the corresponding cytokine in the sham group. Data are expressed as the mean ± SD (n = 5; independent-sample t-test). ###P < 0.001, *vs.* sFWD group. sCCI: Severe controlled cortical impact; sFWD: severe free weight drop; CINC-1: cytokine-induced neutrophil chemoattractant-1; CINC-2α: cytokine-induced neutrophil chemoattractant-2α; CNTF: ciliary neurotrophic factor; CX3CL1: fractalkine; sICAM-1: soluble intercellular adhesion molecule-1; IL-1ra: interleukin-1ra; MIP-1α: macrophage inflammatory protein-1α; CXCL7: thymus chemokine 7; TIMP-1: tissue inhibitor of metalloproteinase-1.

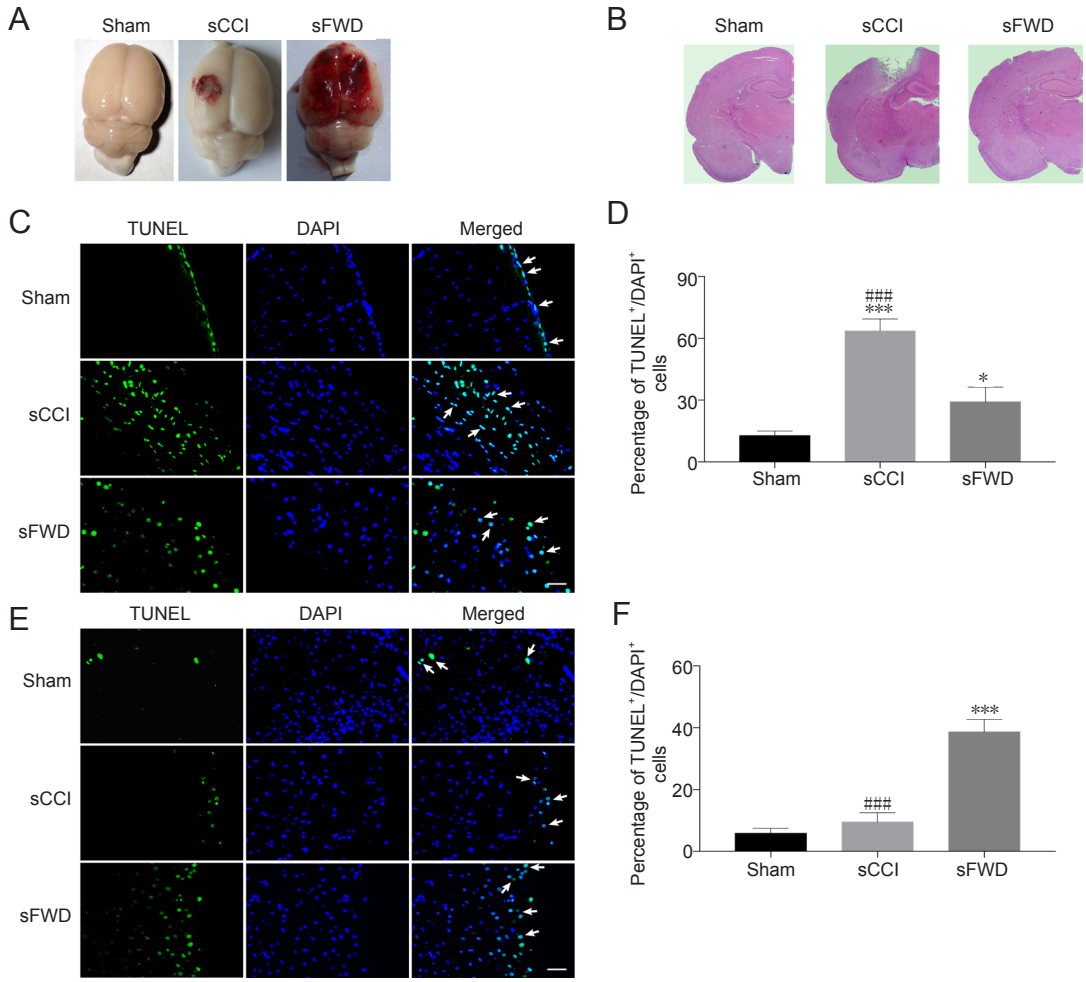

Figure 5 Lesion range, brain neuronal apoptosis and brainstem neuronal apoptosis in rats.
The whole brain raw images (A) and hematoxylin-eosin staining (B) of brain tissue at 72 hours after injury. (C) TUNEL immunofluorescence images around the injured lesion at 72 hours after severe traumatic brain injury. (D) Quantitative analysis of apoptotic cells in the three groups. (E) TUNEL immunofluorescence images in the brainstem at 72 hours after severe traumatic brain injury. (F) Quantitative analysis of apoptotic cells in the three groups. TUNEL: Green; DAPI: blue. Apoptotic cells (arrows) were counted under a fluorescence microscope (original magnification, 400×; scale bar: 200 μm). Data are expressed as the mean ± SD (n = 5; one-way analysis of variance with Bonferroni *post hoc* test). *P < 0.05, ***P < 0.001, *vs.* sham group; ###P < 0.001, *vs.* sFWD group. sCCI: Severe controlled cortical impact; sFWD: severe free weight drop; TUNEL: terminal deoxynucleotidyl transferase-mediated dUTP nick-end labeling; DAPI: 4′,6-diamidino-2-phenylindole.

Discussion

In this study, we compared the neuropathological and functional characteristics of the sCCI and sFWD models of TBI. Both methods produced severe TBI with changes in body temperature, severe neurological impairments, blood-brain barrier damage and neuronal apoptosis. However, there were striking differences between the two models as well.

The sCCI method produces an accurate and reproducible impact. The striking parameters can be controlled, resulting in good repeatability and low mortality (Lighthall, 1988; Dapul et al., 2013). The sFWD model mimics clinical acceleration brain injury, with less structural damage to brain tissue, although it can cause rebound injury and variability in injury severity (Adelson et al., 1996; Kalish and Whalen, 2016). In addition, in the sFWD model, damage not only occurs in the cortex, but also in the cerebellum and brainstem, which leads to vital sign changes and loss of consciousness (Johnson et al., 2015). Accordingly, mortality in sFWD was much higher than in sCCI.

Because neurological dysfunctions in the TBI models are associated with both the degree and location of injury (Bermpohl et al., 2007; Washington et al., 2012), the differences in the sCCI and sFWD models in mNSS reflex and sensory impairment likely result from differences in the degree of injury and/or the lesion area. Diffuse axonal injury, an injury caused by the sFWD model, leads to cognitive and memory dysfunctions (Heath and Vink, 1995; Schmidt et al., 2000). Our current findings are in line with these previous studies. Balance beam test scores in the sFWD group were higher 24 and 72 hours after injury, with a significant difference at 72 hours, compared with the sCCI group. Clinically, even after recovery from diffuse axonal injury, a high proportion of patients show signs of persistent mental retardation (Stewan Feltrin et al., 2018; Aldossary et al., 2019). Cognitive dysfunction in sFWD rats is caused by white matter injury (Filley and Kelly, 2018). In motor tests, only sCCI induced severe dysfunction at 72 hours post injury. It was reported that motor cortex injury leads to impaired motor function (Filley and Kelly, 2018). Our results demonstrate that the cortex in sCCI rats is noticeably damaged, while sFWD produces no obvious damage in hematoxylin-eosin stained sections. This is in accordance with the finding that motor dysfunction is a feature of sCCI, while cognitive dysfunction is a feature of sFWD.

Brain edema, one of the most important risk factors for poor prognosis in TBI, is classified into two types: vasogenic (including blood-brain barrier damage) and cytotoxic (including changes in brain water content) (Nag et al., 2009). Although brain water content was not markedly affected, extensive blood-brain barrier damage in the sFWD group indicated the presence of an inflammatory reaction. In this study, both types of brain edema were observed in the sCCI group, while only vasogenic edema was found in the sFWD group.

Neuroinflammation plays an important role in the mechanisms of secondary brain injury. The pathological process results in the accumulation of peripheral immune cells and the production of a large number of inflammatory cytokines, aggravating brain edema (Simon-O'Brien et al., 2016; Xing et al., 2016; Mishra et al., 2017). Indeed, we found in the present study that a number of inflammatory cytokines were increased in the brain after severe TBI, especially after sCCI. CINC-1 and CINC-2α, cytokines with neutrophil chemotactic activity, aggravate neuroinflammation (Szmydynger-Chodobska et al., 2009). CNTF enhances recovery after neural injury and improves the prognosis of brain injury (Li et al., 2011). However, CNTF can worsen TBI by promoting astrocyte proliferation (Fu et al., 2015). Whether CX3CL1 (fractalkine) and its receptor CX3CR1 are beneficial or harmful after neural injury remains to be clarified (Poniatowski et al., 2017). Upregulation of sICAM-1, which correlates with blood-brain barrier damage, is indicative of an inflammatory reaction (Pleines et al., 1998). IL-1ra, an IL-1 receptor antagonist, inhibits neuroinflammation and reduces brain damage to improve outcome after TBI (Sun et al., 2017). Downregulation of L-selectin decreases inflammation and improves neurological outcome (McCreedy et al., 2018). MIP-1α, CXCL7 and TIMP-1 function as pro-inflammatory cytokines, improving prognosis when downregulated (Cook, 1996; Kobuch et al., 2015; Guo et al., 2017). The inflammatory response after TBI is very complex. Cytokines mediate the inflammatory response to injury (Chiu et al., 2016). While the inflammatory response results in secondary brain damage after injury, it also participates in neural repair to improve prognosis. The inflammatory response can last for months (Xu et al., 2017). However, inflammatory cytokine production in the sFWD model was not significant. The inflammatory response in this model might be delayed and not detectable in the acute and subacute phases.

As described previously (Romine et al., 2014; Zeng et al., 2018), the pathological manifestations of rats with sCCI include hemorrhage in the wound site, focal tissue deformation, neuronal death in the lesion, and increased autophagosomes. In contrast, the sFWD model has two main pathological manifestations: diffuse degeneration and bleeding in the white matter (Chen et al., 1999; Bisht et al., 2013). Indeed, the whole brain images showed significant differences in lesion area between the sCCI and sFWD groups in the present study. The sCCI model featured focal injury, while the sFWD model displayed diffuse injury. Hematoxylin-eosin-stained sections did not reveal a distinct lesion area in the sFWD rats, although these animals had diffuse injuries that are highly relevant to human diffuse axonal injury. Here, apoptotic cells were detected in the brain in both severe TBI models, but only the sFWD model featured brainstem apoptosis. Notably, neuronal apoptosis in the brain was much greater in the sCCI group than in the sFWD group, indicating that sCCI-induced brain injury is more severe than that induced by sFWD.

In this study, we examined the two severe TBI rat models only at the early stage after injury. Neurological function, the inflammatory response and neuronal apoptosis in the middle and late stages of injury were not investigated. In addition, we did not give the area of the lesion or the scale

of the whole brain raw images. We will investigate these in future studies to provide a comprehensive comparison of the sFWD and sCCI models.

In summary, in this study, we examined the differences between the sCCI and sFWD models at the functional, morphological and pathological levels for the first time, laying the foundation for future studies on the different types of severe TBI and to help in the selection of the most appropriate model. Furthermore, these animal models will help to clarify the pathophysiological mechanisms and help in the development of treatments for the various types of severe TBI.

Acknowledgments: *The authors thank Li Liu, Wei-Yun Cui, Fang-Lian Chen, and Lei Zhou from the Key Laboratory of Injuries, Variations and Regeneration of Nervous System, Tianjin Neurological Institute, China for their assistance with the experiments and data analyses.*
Author contributions: *Study design: YMS, WQS, RCJ; experiment implementation: YMS, YQ, XHL; data analysis: JHH, ZTG, HLL; paper writing: YMS; technical support: CG; material support and supervision: RCJ. All authors approved the final version of the paper.*
Conflicts of interest: *The authors declare that there are no conflicts of interest associated with this manuscript.*
Financial support: *This study was supported by the National Natural Science Foundation of China, No. 81671221 (to RCJ). The funding source had no role in study conception and design, data analysis or interpretation, paper writing or deciding to submit this paper for publication.*
Institutional review board statement: *All experimental procedures were approved by the Ethics Committee of Animal Experiments of Tianjin Medical University, China (approval No. IRB2012-028-02) in February 2012.*
Copyright license agreement: *The Copyright License Agreement has been signed by all authors before publication.*
Data sharing statement: *Datasets analyzed during the current study are available from the corresponding author on reasonable request.*
Plagiarism check: *Checked twice by iThenticate.*
Peer review: *Externally peer reviewed.*

Open peer reviewer: *Fabricio Ferreira de Oliveira, Universidade Federal de Sao Paulo, Department of Neurology and Neurosurgery, Brazil.*
Additional file: *Open peer review report 1.*

References

Adelson PD, Robichaud P, Hamilton RL, Kochanek PM (1996) A model of diffuse traumatic brain injury in the immature rat. J Neurosurg 85:877-884.

Aldossary NM, Kotb MA, Kamal AM (2019) Predictive value of early MRI findings on neurocognitive and psychiatric outcomes in patients with severe traumatic brain injury. J Affect Disord 243:1-7.

Bermpohl D, You Z, Lo EH, Kim HH, Whalen MJ (2007) TNF alpha and Fas mediate tissue damage and functional outcome after traumatic brain injury in mice. J Cereb Blood Flow Metab 27:1806-1818.

Bisht A, Garg K, Agarwal D, Singh PK, Satyarthee GD, Gupta D, Sinha S, Kakkar A, Suri V, Lalwani S, Kale SS, Sharma BS (2013) Histological changes in thalamus in short term survivors following traumatic brain injury: an autopsy study. Neurol India 61:599-605.

Buki A, Povlishock JT (2006) All roads lead to disconnection? Traumatic axonal injury revisited. Acta Neurochir (Wien) 148:181-193; discussion 193-184.

Chen X, Chen Y, Xu Y, Gao Q, Shen Z, Zheng W (2018) Microstructural and neurochemical changes in the rat brain after diffuse axonal injury. J Magn Reson Imaging doi: 10.1002/jmri.26258.

Chen XH, Meaney DF, Xu BN, Nonaka M, McIntosh TK, Wolf JA, Saatman KE, Smith DH (1999) Evolution of neurofilament subtype accumulation in axons following diffuse brain injury in the pig. J Neuropathol Exp Neurol 58:588-596.

Chiu CC, Liao YE, Yang LY, Wang JY, Tweedie D, Karnati HK, Greig NH, Wang JY (2016) Neuroinflammation in animal models of traumatic brain injury. J Neurosci Methods 272:38-49.

Clark RS, Schiding JK, Kaczorowski SL, Marion DW, Kochanek PM (1994) Neutrophil accumulation after traumatic brain injury in rats: comparison of weight drop and controlled cortical impact models. J Neurotrauma 11:499-506.

Clausen F, Hillered L (2005) Intracranial pressure changes during fluid percussion, controlled cortical impact and weight drop injury in rats. Acta Neurochir (Wien) 147:775-780.

Cook DN (1996) The role of MIP-1 alpha in inflammation and hematopoiesis. J Leukoc Biol 59:61-66.

Corps KN, Roth TL, McGavern DB (2015) Inflammation and neuroprotection in traumatic brain injury. JAMA Neurol 72:355-362.

Cui DM, Zeng T, Ren J, Wang K, Jin Y, Zhou L, Gao L (2017) KLF4 knockdown attenuates TBI-induced neuronal damage through p53 and JAK-STAT3 signaling. CNS Neurosci Ther 23:106-118.

Dai J, Qiu YM, Ma ZW, Yan GF, Zhou J, Li SQ, Wu H, Jin YC, Zhang XH (2018) Neuroprotective effect of baicalin on focal cerebral ischemia in rats. Neural Regen Res 13:2129-2133.

Dapul HR, Park J, Zhang J, Lee C, DanEshmand A, Lok J, Ayata C, Gray T, Scalzo A, Qiu J, Lo EH, Whalen MJ (2013) Concussive injury before or after controlled cortical impact exacerbates histopathology and functional outcome in a mixed traumatic brain injury model in mice. J Neurotrauma 30:382-391.

Filley CM, Kelly JP (2018) White matter and cognition in traumatic brain injury. J Alzheimers Dis 65:345-362.

Fu XM, Liu SJ, Dan QQ, Wang YP, Lin N, Lv LY, Zou Y, Liu S, Zhou X, Wang TH (2015) Combined bone mesenchymal stem cell and olfactory ensheathing cell transplantation promotes neural repair associated with CNTF expression in traumatic brain-injured rats. Cell Transplant 24:1533-1544.

Gao C, Qian Y, Huang J, Wang D, Su W, Wang P, Guo L, Quan W, An S, Zhang J, Jiang R (2017) A three-day consecutive fingolimod administration improves neurological functions and modulates multiple immune responses of CCI mice. Mol Neurobiol 54:8348-8360.

Gerbatin RDR, Cassol G, Dobrachinski F, Ferreira APO, Quines CB, Pace IDD, Busanello GL, Gutierres JM, Nogueira CW, Oliveira MS, Soares FA, Morsch VM, Fighera MR, Royes LFF (2017) Guanosine protects against traumatic brain injury-induced functional impairments and neuronal loss by modulating excitotoxicity, mitochondrial dysfunction, and inflammation. Mol Neurobiol 54:7585-7596.

Guo F, Ru Q, Zhang J, He S, Yu J, Zheng S, Wang J (2017) Inflammation factors in hepatoblastoma and their clinical significance as diagnostic and prognostic biomarkers. J Pediatr Surg 52:1496-1502.

Heath DL, Vink R (1995) Impact acceleration-induced severe diffuse axonal injury in rats: characterization of phosphate metabolism and neurologic outcome. J Neurotrauma 12:1027-1034.

Johnson VE, Meaney DF, Cullen DK, Smith DH (2015) Animal models of traumatic brain injury. Handb Clin Neurol 127:115-128.

Jullienne A, Obenaus A, Ichkova A, Savona-Baron C, Pearce WJ, Badaut J (2016) Chronic cerebrovascular dysfunction after traumatic brain injury. J Neurosci Res 94:609-622.

Kalish BT, Whalen MJ (2016) Weight drop models in traumatic brain injury. Methods Mol Biol 1462:193-209.

Kobuch J, Cui H, Grunwald B, Saftig P, Knolle PA, Kruger A (2015) TIMP-1 signaling via CD63 triggers granulopoiesis and neutrophilia in mice. Haematologica 100:1005-1013.

Kulbe JR, Singh IN, Wang JA, Cebak JE, Hall ED (2018) Continuous infusion of phenelzine, cyclosporine A, or their combination: evaluation of mitochondrial bioenergetics, oxidative damage, and cytoskeletal degradation following severe controlled cortical impact traumatic brain injury in rats. J Neurotrauma 35:1280-1293.

Li R, Wen R, Banzon T, Maminishkis A, Miller SS (2011) CNTF mediates neurotrophic factor secretion and fluid absorption in human retinal pigment epithelium. PLoS One 6:e23148.

Lighthall JW (1988) Controlled cortical impact: a new experimental brain injury model. J Neurotrauma 5:1-15.

Lin HJ, Hsu CC, Chio CC, Tian YF, Lin MT, Lin TW, Chang CH, Chang CP (2017) Gamma-secretase inhibitors attenuate neurotrauma and neurogenic acute lung injury in rats by rescuing the accumulation of hypertrophic microglia. Cell Physiol Biochem 44:1726-1740.

Ma X, Aravind A, Pfister BJ, Chandra N, Haorah J (2019) Animal models of traumatic brain injury and assessment of injury severity. Mol Neurobiol doi: 10.1007/s12035-018-1454-5.

Marmarou A, Foda MA, van den Brink W, Campbell J, Kita H, Demetriadou K (1994) A new model of diffuse brain injury in rats. Part I: Pathophysiology and biomechanics. J Neurosurg 80:291-300.

Mateo Z, Porter JT (2007) Group II metabotropic glutamate receptors inhibit glutamate release at thalamocortical synapses in the developing somatosensory cortex. Neuroscience 146:1062-1072.

McCreedy DA, Lee S, Sontag CJ, Weinstein P, Olivas AD, Martinez AF, Fandel TM, Trivedi A, Lowell CA, Rosen SD, Noble-Haeusslein LJ (2018) Early targeting of L-selectin on leukocytes promotes recovery after spinal cord injury, implicating novel mechanisms of pathogenesis. eNeuro doi: 10.1523/ENEURO.0101-18.2018.

Mishra SK, Kumar BS, Khushu S, Singh AK, Gangenahalli G (2017) Early monitoring and quantitative evaluation of macrophage infiltration after experimental traumatic brain injury: a magnetic resonance imaging and flow cytometric analysis. Mol Cell Neurosci 78:25-34.

Nag S, Manias JL, Stewart DJ (2009) Pathology and new players in the pathogenesis of brain edema. Acta Neuropathol 118:197-217.

Obenaus A, Ng M, Orantes AM, Kinney-Lang E, Rashid F, Hamer M, DeFazio RA, Tang J, Zhang JH, Pearce WJ (2017) Traumatic brain injury results in acute rarefication of the vascular network. Sci Rep 7:239.

Ogata M (2007) Early diagnosis of diffuse brain damage resulting from a blunt head injury. Leg Med (Tokyo) 9:105-108.

Osier N, Dixon CE (2016a) The controlled cortical impact model of experimental brain trauma: overview, research applications, and protocol. Methods Mol Biol 1462:177-192.

Osier ND, Dixon CE (2016b) The controlled cortical impact model: applications, considerations for researchers, and future directions. Front Neurol 7:134.

Pleines UE, Stover JF, Kossmann T, Trentz O, Morganti-Kossmann MC (1998) Soluble ICAM-1 in CSF coincides with the extent of cerebral damage in patients with severe traumatic brain injury. J Neurotrauma 15:399-409.

Poniatowski LA, Wojdasiewicz P, Krawczyk M, Szukiewicz D, Gasik R, Kubaszewski L, Kurkowska-Jastrzebska I (2017) Analysis of the role of CX3CL1 (fractalkine) and its receptor CX3CR1 in traumatic brain and spinal cord injury: insight into recent advances in actions of neurochemokine agents. Mol Neurobiol 54:2167-2188.

Povlishock J (2016) The history and evolution of experimental traumatic brain injury models. Methods Mol Biol 1462:3-7.

Romine J, Gao X, Chen J (2014) Controlled cortical impact model for traumatic brain injury. J Vis Exp doi:10.3791/51781.

Schmidt RH, Scholten KJ, Maughan PH (2000) Cognitive impairment and synaptosomal choline uptake in rats following impact acceleration injury. J Neurotrauma 17:1129-1139.

Simon-O'Brien E, Gauthier D, Riban V, Verleye M (2016) Etifoxine improves sensorimotor deficits and reduces glial activation, neuronal degeneration, and neuroinflammation in a rat model of traumatic brain injury. J Neuroinflammation 13:203.

Stewan Feltrin F, Zaninotto AL, Guirado VMP, Macruz F, Sakuno D, Dalaqua M, Magalhaes LGA, Paiva WS, Andrade AF, Otaduy MCG, Leite CC (2018) Longitudinal changes in brain volumetry and cognitive functions after moderate and severe diffuse axonal injury. Brain Inj 32:1208-1217.

Su Y, Fan W, Ma Z, Wen X, Wang W, Wu Q, Huang H (2014) Taurine improves functional and histological outcomes and reduces inflammation in traumatic brain injury. Neuroscience 266:56-65.

Sun M, Brady RD, Wright DK, Kim HA, Zhang SR, Sobey CG, Johnstone MR, O'Brien TJ, Semple BD, McDonald SJ, Shultz SR (2017) Treatment with an interleukin-1 receptor antagonist mitigates neuroinflammation and brain damage after polytrauma. Brain Behav Immun 66:359-371.

Szmydynger-Chodobska J, Strazielle N, Zink BJ, Ghersi-Egea JF, Chodobski A (2009) The role of the choroid plexus in neutrophil invasion after traumatic brain injury. J Cereb Blood Flow Metab 29:1503-1516.

Washington PM, Forcelli PA, Wilkins T, Zapple DN, Parsadanian M, Burns MP (2012) The effect of injury severity on behavior: a phenotypic study of cognitive and emotional deficits after mild, moderate, and severe controlled cortical impact injury in mice. J Neurotrauma 29:2283-2296.

Xing Z, Xia Z, Peng W, Li J, Zhang C, Fu C, Tang T, Luo J, Zou Y, Fan R, Liu W, Xiong X, Huang W, Sheng C, Gan P, Wang Y (2016) Xuefu Zhuyu decoction, a traditional Chinese medicine, provides neuroprotection in a rat model of traumatic brain injury via an anti-inflammatory pathway. Sci Rep 6:20040.

Xu X, Gao W, Cheng S, Yin D, Li F, Wu Y, Sun D, Zhou S, Wang D, Zhang Y, Jiang R, Zhang J (2017) Anti-inflammatory and immunomodulatory mechanisms of atorvastatin in a murine model of traumatic brain injury. J Neuroinflammation 14:167.

Zeng XJ, Li P, Ning YL, Zhao Y, Peng Y, Yang N, Zhao ZA, Chen JF, Zhou YG (2018) Impaired autophagic flux is associated with the severity of trauma and the role of A2AR in brain cells after traumatic brain injury. Cell Death Dis 9:252.

P-Reviewer: Ferreira de Oliveira F; C-Editor: Zhao M; S-Editors: Wang J, Li CH; L-Editors: Patel B, Yajima W, Qiu Y, Song LP; T-Editor: Jia Y